International Journal of Transport Development and Integration
https://www.acadlore.com/journals/IJTDI

# Monitoring Irregularities of the Longitudinal Profile Railway Track by Using Accelerometer Data Mounted in the Train Cabin

Istiar, Hera Widyastuti*

Department of Civil Engineering, Institut Teknologi Sepuluh Nopember, ITS Campus Sukolilo Surabaya, 60111 Surabaya, Indonesia

* Correspondence: Hera Widyastuti (hera@ce.its.ac.id)

**Received:** 06-05-2025 **Revised:** 08-01-2025 **Accepted:** 08-05-2025

**Citation:** Istiar and H. Widyastuti, "Monitoring irregularities of the longitudinal profile railway track by using accelerometer data mounted in the train cabin," *Int. J. Transp. Dev. Integr.*, vol. 9, no. 4, pp. 870–885, 2025. https://doi.org/10.56578/ijtdi090413.



**Abstract:** The purpose of the research was to find out the most efficient method to measure the longitudinal profile irregularities of the railway track geometry. Some researchers used an accelerometer installed at the axle-box bogie to monitor the longitudinal profile of the railway track. However, the method was risky because the accelerometer could disappear due to improper installation. In this research, the accelerometer was installed in the train cabin. The scope of analysis started with the IMU calibration by manual technique, filtering the Z-axis acceleration of IMU data by the Kalman Filter method, and converting to longitudinal profile data by double integral calculation. The normal distribution of the longitudinal profile of the railway track based on the acceleration data and measurement data of the track geometry measuring train (TGMT) was tested by the Kolmogorov-Smirnov Method. The paired comparison test used the Wilcoxon signed-ranks test method, and test results showed the P-value is 0.725 (left rail) and 0.073 (right rail), which are greater than 0.05. Therefore, no difference between the longitudinal profile based on the TGMT data and the longitudinal profile based on accelerometer data analysis, and the longitudinal profile irregularities can be monitored by using the accelerometer in the train cabin. The use of this method will support SDGs 9, build resilient infrastructure.

**Keywords:** Longitudinal profile; Track geometry measuring train; Z-axis acceleration; IMU calibration; Kalman Filter; Kolmogorov-Smirnov; Wilcoxon signed-ranks test; SDGs 9

## 1 Introduction

The railways had the advantage of having their track, with two parallel rails set at a certain distance [1]. With this advantage, railways are relatively free from congestion compared to road infrastructure [2, 3] and occupy 2–3 times less land per passenger than other modes of road transport [4]. When compared to airplanes, trains have the advantage of producing fewer emissions [5]. The railway line capacity will increase if the railway line has double-track construction [6]. Railway is one of the land transportation infrastructures, besides road transportation. The train, as a mode of railway transportation, has been the most popular land transportation mode in Indonesia [7].

Currently, the railway maintenance system in Indonesia is based on the Track Quality Index (TQI) [8]. The TQI was a value derived from measuring the geometric conditions of railway tracks using the track geometry measuring train (TGMT) at 25 cm intervals along the railway length. One of the measuring geometry trains operated in Indonesia is shown in Figure 1. The use of TGMT to acquire railroad quality data was accompanied by several disadvantages. Utilizing a measuring geometry train for measurements would incur relatively high costs. Apart from requiring high costs, checking the geometry condition of the railroad using a measuring geometry train will potentially disrupt the commercial train schedule that has been prepared [9, 10]. The operation of the TGMT will adjust to the commercial train travel schedule that has been prepared. Consequently, the frequencies of the TGMT inspections are relatively low, potentially leading to undetected geometry problems on the railway. During the rainy season, the optical laser sensor equipment on the measuring geometry train typically experiences interference due to environmental conditions in the structure beneath the railroad [11]. Overall, the use of the TGMT for the measurement of railway track geometry was not efficient.

**Figure 1.** TGMT in Indonesia

Railway infrastructure must ensure the safety of train travel. The Ministry of Transportation's Transportation Information Book (BIT) 2022 reports that derailments caused 62 out of 71 railway transportation accidents in Indonesia, accounting for 87.33% of these incidents [12]. The geometric condition of the railway track was identified as one of the causes of derailments [13]. These accidents caused disruptions in train travel. Efficient maintenance policies, based on risk assessment for various infrastructure components, are necessary to anticipate potential problems in railway infrastructure and prevent train travel disruptions [14].

## 2 Literature Review

The dynamic response of a train cabin was the movement of the train cabin structure as a reaction, one of which was caused by irregularity of the railway track. The dynamic response that occurs in a train cabin can be detected from the changes in the train cabin acceleration. The changes in train cabin acceleration were measured by an accelerometer. An accelerometer was a sensor tool that was used for acceleration measurement, and it was one type of inertial measurement unit (IMU). An IMU is an automatic tool for measuring acceleration, detecting and measuring vibration, and measuring acceleration due to the body's inclination [15]. IMU becomes IMMU when it incorporates a magnetometer [16]. In this research, the type of accelerometer used was an accelerometer that was part of the micro-electromechanical system (MEMS).

Installing accelerometers on operating trains allows for the monitoring of the railway geometry condition, providing valuable information [11, 17–19]. Furthermore, this method does not require human power when operated concurrently with train operations [18]; therefore, the costs are relatively low [20].

Acceleration refers to the change in an object's speed over time. Acceleration occurred when the speed increased over time, and deceleration occurred when the speed decreased. However, deceleration occurred when the speed dropped from its previous level. Acceleration was also dependent on the direction or orientation, as it reduced the velocity of the vector. Changes in the direction of objects would also result in acceleration.

Several IMU sensor tools and methods were developed to check railway conditions more effectively and efficiently. An accelerometer was one of the IMUs that was frequently used to predict railway geometry conditions. Chudzikiewicz et al. [17] used an accelerometer on the axle-box of a bogie train. The study took place in Poland, and the TQI value that was found by analyzing the accelerometer data was compared to other railway quality indicators, specifically W5 and J Synthetic. Real et al. [18] mounted an accelerometer on a train's bogie axle-box to predict the longitudinal profile of a railway track. The prediction results of the railway longitudinal profile, which relied on accelerometer data, were compared with the longitudinal profile of the railroad track using trolley measurements. The research was conducted in Spain.

Weston et al. [11] installed an accelerometer and pitch-rate gyro on the bogie axle-box of the UK's Tyne and Wear Metro. These IMU data were compared with vertical profile data from the Track Record Vehicle (TRV) measurement 16 months earlier. Xing et al. [21] also used the IMU (pitch rate gyro) to monitor irregularities in the longitudinal vertical profile of the railway online. The study used only one type of IMU, specifically the bogie pitch-rate IMU. The results of the IMU measurements would be tested and compared with the actual conditions of irregularities in the vertical profile of the rail, which were obtained from measurements of China's high-speed trains. Obrien et al. [22] recorded vertical acceleration data and the angular speed of a train bogie using an IMU. The collected IMU data was used to predict the longitudinal profile of the railway using the cross-entropy optimization method. The research location was in Ireland, specifically on the Irish Rail Hyundai Rotem InterCity train.

Train axle-boxes install accelerometers to optimize measurement results for railway condition monitoring [23]. The analysis utilized mathematical models and the accelerometer data's dynamic frequency response. The research location was in India, which had a 1676-millimeter track gauge. Nadarajah et al. [24] conducted the research in Indonesia on the northern Surabaya - Lamongan railway line, using several IMUs to predict railway geometry

parameters such as longitudinal, lateral, and cross-level profiles, based on the dynamic response behavior of IMUs installed at various train locations such as axle boxes, bogies, and carriages.

Accelerometers were also used to measure the comfort level of railway passengers (Passenger Ride Comfort, PRC) [25]. The object study was the railway track between Tehran to Mashhad, which is located in the central part of Iran. The length of the railway is about 114 km and has a high density of train traffic. An IMU was also used for comfort assessment [26]. The experiment was done in electric multiple units, called Alstom Metropolis 98 B. The measurements were recorded during the trip between the Marymont station to the Rac lawicka station. Three locations, the front, back, and middle of the vehicle, were selected.

Previous researchers had studied using accelerometers to monitor longitudinal profile, in which the accelerometers were mostly located at the axle-box of the train bogie. However, placing the IMU sensor in the axle-box of the train bogie has the potential to fall or be lost due to installation errors [14]. Another researcher had used the accelerometers in the train cabin, but the purpose was to monitor the comfort level of railway passengers. The summary of the literature study above will be shown in Table 1.

**Table 1.** Previous research on accelerometers used on an in-service train

| Sensor Location | The Research Purposes | Reference |
|---|---|---|
| Axel-Box Train Bogie | TQI value | [17] |
| Axel-Box Train Bogie | To predict the Longitudinal Profile | [18] |
| Axel-Box Train Bogie | To compare with vertical profile data from the TRV | [14] |
| Axel-Box Train Bogie | To monitor irregularities in the longitudinal vertical profile of the railway | [19] |
| Axel-Box Train Bogie | To predict the longitudinal profile of the railway using the cross-entropy optimization method | [22] |
| Axel-Box Train Bogie | To optimize measurement results for railway condition monitoring | [23] |
| Axel-Box Train Bogie | To predict railway geometry parameters such as longitudinal, lateral, and cross-level profiles | [24] |
| In the train cabin | To measure the comfort level of railway passengers (Passenger Ride Comfort, PRC) | [25] |
| In the train cabin | To assess train comfort | [26] |

## 3 Limitation of Study

Due to limited information on the measurement data obtained and the sensor module in the IMU, this research will be limited to the following: There was no sensitivity analysis for calibration drift over time and temperature-induced MEMS bias.

## 4 Methodology

The research started with a literature study. The next step was data collection. The secondary data collected was the vertical alignment or longitudinal profile of the railway track data from the track geometry measurement train. The acceleration data of the train cabin was the primary data that had been collected in this research.

The primary data had to be calibrated because the acquisition of the primary data had errors in scaling, offset, and accelerometer-axis errors. The acceleration data of the train cabin that had been calibrated was filtered by using the Kalman Filter Method. The next step of analysis converted the filtered acceleration data into longitudinal profile data by double integration calculation.

The final step of the research compares the longitudinal profile data of the railway track based on the acceleration data of the train cabin with the longitudinal profile data of the railway track based on the TGMT. Both longitudinal profile data of the railroad track have been checked for normality of data distribution before being compared. Normality data testing uses the Kolmogorov-Smirnov Method. If neither of the data sets is normal, the comparison analysis will use the Student T-test, and vice versa, will use the Wilcoxon Signed Rank Test.

### 4.1 Calibrating the Acceleration Data of the IMU

In this research, the IMU sensor tool used a micro-electromechanical system (MEMS). The use of MEMS as an IMU had many errors that affected on IMU measurement [27]. Acceleration data of the train cabin should be calibrated by multiplying by the calibrating factor of the IMU sensor tool. Acceleration train cabin data should be calibrated because the acquisition data of the IMU sensor tool did not record actual acceleration due to many factors. The factors that affected of IMU measurement result were scaling error, offset error, non-orthogonality of accelerometer axis error, etc. The calibrating factor of the IMU sensor tool was obtained in a simple method by a mathematical model [28].

A simple procedure to calibrate accelerometer data measurements was to put the IMU device in six standard positions. Additional requirements for implementing a simple accelerometer calibration procedure are six standard positions in a stable and flat environment. To obtain six standard positions in a stable and flat position, we used a table, a floor, and a window frame. The IMU device measured acceleration data for several seconds, and the results were averaged; therefore, the noise that occurs during the measurement for calibration would be reduced. The IMU device acceleration data vector from the measurement results for calibration or in six standard positions were $m^{(1)}$, $m^{(2)}$, $m^{(3)}$, $m^{(4)}$, $m^{(5)}$, $m^{(6)}$, while an actual acceleration data in six standard positions were $a^{(1)}$, $a^{(2)}$, $a^{(3)}$, $a^{(4)}$, $a^{(5)}$, $a^{(6)}$ where the value was equal as the earth's gravitational force. An illustration of the six standard positions for the acceleration data calibration process from the IMU device can be seen in Figure 2.

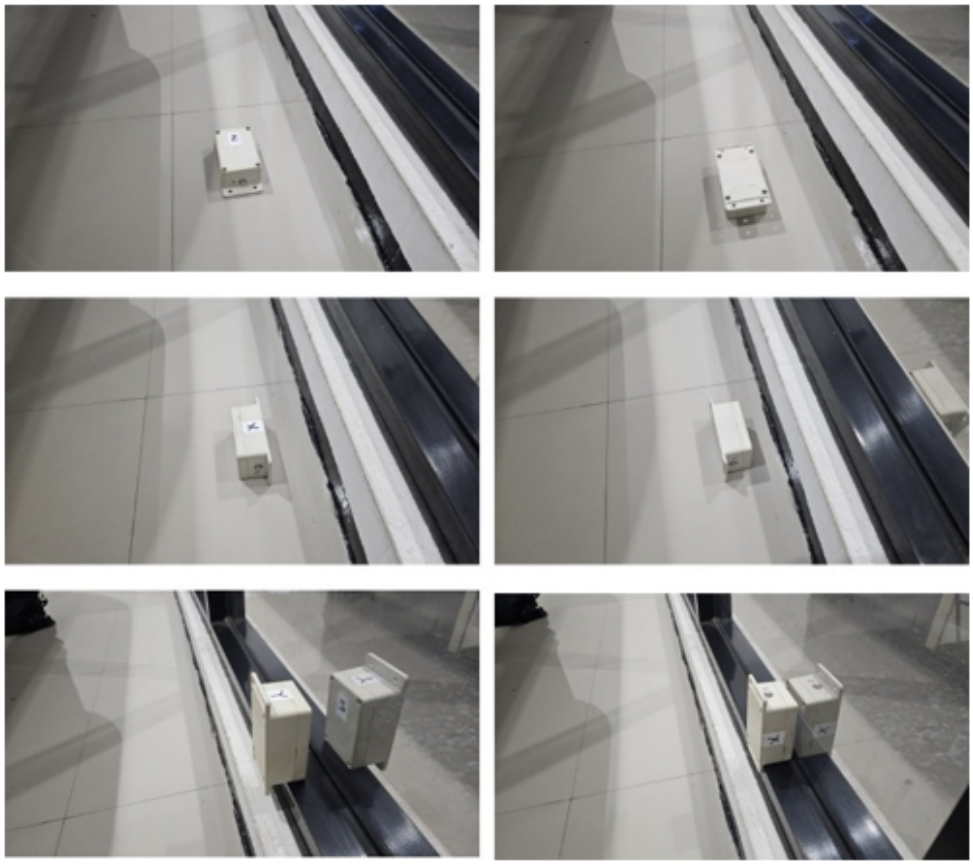

**Figure 2.** Six standard positions of the IMU tool for calibration measurement

If the measured acceleration data vector, $m$ = ($m_x$, $m_y$, $m_z$), and the actual acceleration data vector, $a$ = ($a_x$, $a_y$, $a_z$), then the relationship between the measured acceleration data vector and the actual acceleration data vector is as follows.

$$m = X_a + y \tag{1}$$

where, $m$ is the measurement acceleration, $a$ is the actual acceleration, $X$ is the scaling error, and $y$ is the offset or bias.

The actual acceleration data ($a$) resulted from the inverse operation of the measurement data ($m$) and can be seen in Eq. (1) by computing $X$ and $y$:

$$a = X^{-1}(m - y) \tag{2}$$

Eq. (2) has 12 variables, consisting of 9 variables of $X$ and 3 variables of $y$. Eq. (1) had broken down into component form:

$$X_{11} * a_1 + X_{12} * a_2 + X_{13} * a_3 + y_1 = m_1 \tag{3}$$

$$X_{21} * a_1 + X_{22} * a_2 + X_{23} * a_3 + y_2 = m_2 \tag{4}$$

$$X_{31} * a_1 + X_{32} * a_2 + X_{33} * a_3 + y_3 = m_3 \tag{5}$$

Variables $X$ and $y$ were unknown, and if combined into an unknown single vector $Z \in R^{12}$, that was,

$$Z = (X_{11}, X_{12}, X_{13}, X_{21}, X_{22}, X_{23}, X_{31}, X_{32}, X_{33}, y_1, y_2, y_3)^T \tag{6}$$

If Eqs. (1)–(6) are written in the form of matrix equations, which become as follows:

$$\begin{pmatrix} a_1 & a_2 & a_3 & 0 & 0 & 0 & 0 & 0 & 0 & 1 & 0 & 0 \\ 0 & 0 & 0 & a_1 & a_2 & a_3 & 0 & 0 & 0 & 0 & 1 & 0 \\ 0 & 0 & 0 & 0 & 0 & 0 & a_1 & a_2 & a_3 & 0 & 0 & 1 \end{pmatrix} z = m \tag{7}$$

If the matrix in the Eq. (7) by $K(a) \in R^{3^{\times}12}$, Eq. (7) was written shortly:

$$K(a)z = m \tag{8}$$

Eqs. (3)–(5) were linear equations with 12 unknown variables, but only 3 equations, and therefore, they could not be determined. To find a solution, it was necessary to take multiple measurements ($m$) for different actual accelerations ($a$). The comparison of the actual accelerometer data vector and the measurement data vector was written as follows:

$$a^{(1)} = \left(a_x^{(1)}, a_y^{(1)}, a_z^{(1)}\right), m^{(1)} = \left(m_x^{(1)}, m_y^{(1)}, m_z^{(1)}\right)$$

$$\vdots$$

$$a^{(N)} = \left(a_x^{(N)}, a_y^{(N)}, a_z^{(N)}\right), m^{(N)} = \left(m_x^{(N)}, m_y^{(N)}, m_z^{(N)}\right)$$

Eq. (9) was a linear equation matrix after $N$ frequency measurements based on Eq. (8).

$$\begin{bmatrix} K\left(a^{(1)}\right) \\ K\left(a^{(2)}\right) \\ \vdots \\ K\left(a^{(N)}\right) \end{bmatrix} z = \begin{bmatrix} m^{(1)} \\ m^{(2)} \\ \vdots \\ m^{(N)} \end{bmatrix} \tag{9}$$

The matrix on the left side of Eq. (9) was ($K$), had size 3 $N \times 12$, and the matrix on the right side of Eq. (9) was ($m$), had a vector of size 3 $N$. Eq. (9) was written as a new equation as below:

$$Kz = \overline{m}$$

If the measurement was done 4 times, the linear equation system becomes square and would produce four vectors for its solution:

$$\left(a_x^{(i)} \quad a_y^{(i)} \quad a_z^{(i)} \quad 1\right), i = 1, 2, 3, \ldots, n \tag{10}$$

It was recommended to take more than 3 times of measurements, at least 6 measurements at six standard positions (see Figure 2). Therefore, the linear equation system in Eq. (8) can be analyzed using the Least Squares Method.

$$K^T K z = K^T \bar{m} \tag{11}$$

The summary of the actual six standard positions of accelerometer data was:

$$a^{(1)} = (-g, 0, 0), a^{(3)} = (0, -g, 0), a^{(5)} = (0, 0, -g),$$
$$a^{(2)} = (g, 0, 0), a^{(4)} = (0, g, 0), a^{(6)} = (0, 0, g).$$

Making a diagonal matrix out of the least squares matrix was a simple method for this, where:

$$K^{\top}K = \operatorname{diag}\left(2g^2, 2g^2, 2g^2, 2g^2, 2g^2, 2g^2, 2g^2, 2g^2, 2g^2, 6, 6, 6\right).$$

Therefore, the least squares method problem of Eq. (1) had a simple solution as follows:

$$X = \frac{1}{2g}\begin{pmatrix} -m_x^{(1)} + m_x^{(2)} & -m_x^{(3)} + m_x^{(4)} & -m_x^{(5)} + m_x^{(6)} \\ -m_y^{(1)} + m_y^{(2)} & -m_y^{(3)} + m_y^{(4)} & -m_y^{(5)} + m_y^{(6)} \\ -m_z^{(1)} + m_z^{(2)} & -m_z^{(3)} + m_z^{(4)} & -m_z^{(5)} + m_z^{(6)} \end{pmatrix} \tag{12}$$

$$y = \frac{1}{6}\sum_{i=1}^{6}\begin{bmatrix} {m_x}^{(i)} \\ {m_y}^{(i)} \\ {m_z}^{(i)} \end{bmatrix} \tag{13}$$

Therefore, in this case, calibration does not need an inverted matrix process. But just a simple arithmetic calculation was required to find out the scaling factor and the offset for the calibration of train cabin acceleration data. This process was very cheap in computation and was done without additional software on the IMU device. The accuracy verification of the IMU calibration is done by comparing the actual train travel length and the double integral analysis of the Y-axis acceleration data.

### 4.2 The Kalman Filter Method

Every sensor device has noise or interference that can affect the result of the measurement. In this study, noise filtering would use the Standard Kalman Filter because it consisted of sufficient equations for reducing noise. The Kalman filter was a popular method for noise filtering because it had easy computation and low memory requirements [29]. Rudolf E. Kalman proposed the Kalman Filter in 1960 [30] and applied it to many fields, including tracking objects [31] and navigation systems [32]. The various methods of the Kalman Filter were the Standard Kalman Filter [33], Extended Kalman Filter [34], Unscented Kalman Filter [35], and Ensemble Kalman Filter [36]. The simplest approach of the Kalman Filter was the standard Kalman Filter, because the other approaches were adjusted for more complicated computations. The predictions and correct equations in the Kalman filter were shown in Eqs. (14)–(18) [29]:

Predict:

$$\hat{x}_{t|t-1} = F_t\hat{x}_{t-1|t-1} + B_tU_t \tag{14}$$

$$P_{t|t-1} = F_tP_{t-1|t-1}F_t^T + Q_t \tag{15}$$

Correct:

$$\hat{x}_{t|t-1} = \hat{x}_{t-1|t-1} + K_t\left(y_t - H_t\hat{x}_{t|t-1}\right) \tag{16}$$

$$K_t = P_{t|t-1}H_t^T\left(H_tP_{t|t-1}H_t^T + R_t\right)^{-1} \tag{17}$$

$$P_{t|t} = \left(I - K_tH_t\right)P_{t|t-1} \tag{18}$$

where, $x$ was a predicted state, a state transition matrix was $F$, $u$ was a control variable, a control matrix was $B$, $H$ was a measurement matrix, a measurement variable was $y$, $T$ was a process variance matrix, a state variance matrix was $P$, $K$ is a Kalman filter gain, the process variance matrix was $Q$, $R$ is a measurement variance matrix, $t \mid t$ is current time period, $t$ - 1 $\mid$ $t$ - 1 is prevoius time period, and $t \mid t$ - 1 is intermediate step. The Kalman Filter Process Model was shown in Figure 3.

The Kalman filter parameters are set when predicting conditions at the start of the process using Eq. (14), with $F$ = 1. Control variables $B$ and $U$ are not used. Both are set to 0. The Kalman Gain calculation can be performed using Eq. (17) to adjust for $H$ = 1.

### 4.3 Space-Domain Track Longitudinal Irregularity Displacement Calculation

The acceleration data of the train cabin must be converted to vertical or longitudinal profile data of the railway track by multiple integrals on the acceleration data of the train cabin [19]. Therefore, it could be compared with the longitudinal profile data of a railway track obtained by TGMT. The formula of multiple integrals converted the acceleration data of the train cabin to longitudinal profile data is shown in Eq. (19):

$$\hat{z}_a = \iint a_z dtdt = \iint \frac{a_z}{v_z^2} dsds \tag{19}$$

where, $\hat{z}_a$ was the Z-axis position, $a_z$ was Z-axis acceleration, $t_1$ was time, $v_z$ was Z-axis velocity, and $s$ was distance.

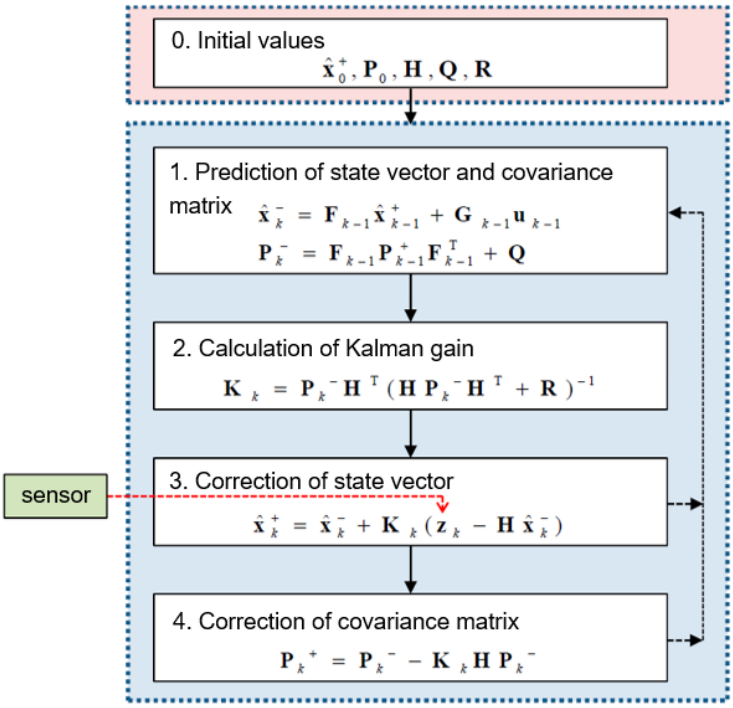


**Figure 3.** Kalman filter process model [37]

### 4.4 Statistical Analysis

Statistical Analysis was taken by comparing the mean of the longitudinal profile railway track data of measuring TGMT with the mean of the longitudinal profile railway track based on the acceleration data of the train cabin. Both data sets will be analyzed statistically to determine whether the data are paired or not; it is called a paired 2-sample dependent test [38]. There were 2 types of statistical analysis mentioned above, Student's T-test and Wilcoxon Signed Ranks Test. Student's T-test will be used if the TGMT data and train cabin acceleration data are in normal distribution [39]. The formula of Student's T-test was shown in Eq. (20):

$$t = \frac{Z}{s} = \frac{\bar{X} - \mu}{\hat{\sigma}/\sqrt{n}} \tag{20}$$

where, $\bar{X}$ was the mean of a sample $X1$, $X2$, ..., $Xn$, of size $n$ , $s$ was the standard error of the mean, $\hat{s}$ was the standard deviation of the population, and $\mu$ was the mean of the population. The result of the Student's T-test can be determined based on:

a. P-value or Significant value (2-tailed) $> \alpha$ value, then $H_0$ is accepted.

b. P-value or Significant value (2-tailed) $< \alpha$ value, then $H_0$ is rejected and $H_1$ is accepted.

The Wilcoxon Signed Rank Test was a non-parametric test to determine the difference in the average of paired 2 samples with non-normally distributed data [40]. This test was an alternative test to the Student's T-test if the data were not normally distributed. The Wilcoxon Signed Ranks Test formula is as Eq. (21):

$$Z = \frac{J - \mu_J}{\sigma_J} = \frac{J - \frac{n(n+1)}{4}}{\sqrt{\frac{n(n+1)(2n+1)}{24}}} \tag{21}$$

where, $Z$ is the normal test count, $J$ is the number of small levels or ranks, $\mu_J$ is the average level/rank, and $s_J$ is the standard deviation of ranking levels.

The result of the Wilcoxon Test can be determined based on probability (Asymptotic Significance), namely:

a. P-value or asymptotic significance value (2-tailed )$> \alpha$ value, then $H_0$ was accepted.

b. P-value or asymptotic significance value (2-tailed) $< \alpha$ value, then $H_0$ was rejected and $H_1$ was accepted.

#### 4.4.1 Normality data testing

The first step of statistical analysis was to test the distribution of both datasets, whether normal or not normal. If both datasets were normally distributed, the method of statistical analysis was the Student T-test. However, if both datasets were not normally distributed, the method of statistical analysis was the Wilcoxon Signed Rank Test.

Normality data testing used the Kolmogorov-Smirnov Method. The null hypothesis of normality data testing was that the sample data had a normal distribution. The data was in normal distribution if the P-value or asymptotic significance (2-tailed) value was more than 0.05.

#### 4.4.2 Null hypothesis testing

The initial step in a two-sample pair of samples was to determine the null hypothesis of the statistical test. In this research, the null hypothesis was that there was no difference between the longitudinal profile railway data based on the acceleration data of the train cabin and the longitudinal profile railway data based on the TGMT measurement; vice versa, for the alternate hypothesis, the profile railway track data based on TGMT and the profile railway track data based on the train cabin's acceleration data differed. The method was used to test two dependent pairs of samples that were Student's T-test or the Wilcoxon Signed Rank Test, depending on data distribution (normal or not).

## 5 Results and Discussion

### 5.1 Data Collection

The primary data collected in this research were dynamic response data in a train cabin. The dynamic response data that would be used was the train cabin acceleration. The collection of train cabin acceleration data, using an IMU sensor, consists of an accelerometer, a gyroscope, a GPS, and a time. The GPS and time acquisition were used to verify the calculation result in the analysis stage. The IMU sensor was installed on the floor of the train cabin (see Figure 4). The data of the IMU sensor tool used for this research was Z-axis acceleration data. The sample rate of the IMU was set to 200 Hz, and the average speed of the train was 54 km/h or 15 m/s. Therefore, the corrected sampling rate of the IMU was recorded every 7.5 cm. The acceleration data on the left railway in the train cabin was shown in Figure 5, and Figure 6 showed the acceleration data on the right railway track.

**Figure 4.** The installation of the IMU sensor tool

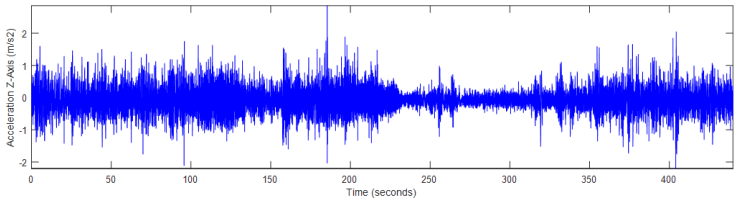


**Figure 5.** The acceleration data of the train cabin on the left rail of the Bandung to Rancaekek line, Kilometer 161+000–Kilometer 168+000

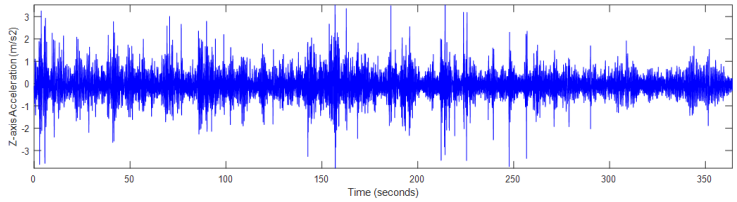


**Figure 6.** The acceleration data of the train cabin on the right rail of the Bandung to Rancaekek line, Kilometer 161+000–Kilometer 168+000

Another data required in this research was the longitudinal railway profile, which was the result of the geometry measurement of the railway by the TGMT. The railway track segment was chosen in the research, which was between Bandung to Rancaekek, KM 161+000—KM 168+000, which was a 7 km long segment (see Figure 7). The speed of

the TGMT that was recorded in the document of the survey report was 65.31 km/h. The selection of sample locations for the railway track segments should consider straight track, and the time interval between TGMT measurements and IMU measurements should not be too long. Figures 8 and 9 show the longitudinal irregularity of railway track data based on the geometry measuring train.

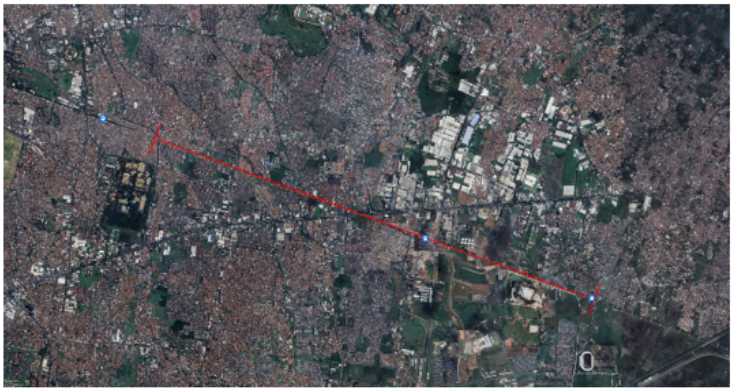

**Figure 7.** The research location

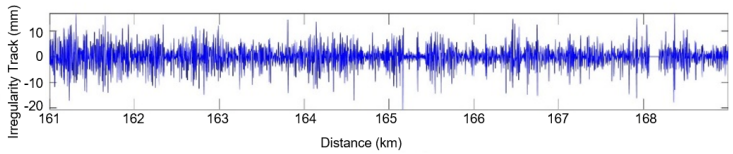


**Figure 8.** The irregularity of the left-side longitudinal profile railway track between Bandung to Rancaekek, Kilometer 161+000–Kilometer 168+000

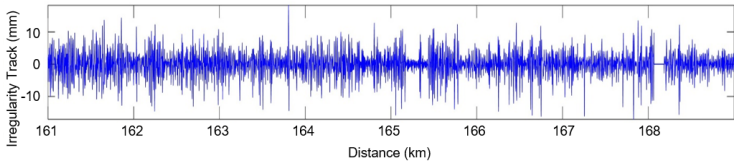


**Figure 9.** The irregularity of the right-side longitudinal profile railway track between Bandung to Rancaekek, Kilometer 161+000–Kilometer 168+000

### 5.2 Determination of Calibrating Parameter

As mentioned above (Section 3.1), acceleration data from train cabin data acquisition should be calibrated because the acquisition data of the IMU sensor tool in the train cabin did not record true physical acceleration due to many factors, including errors on scaling, offset, and non-orthogonality of the accelerometer axes, and noise that occurs during measurement. There were 2 parameters of calibration: the scale factor and the bias or offset value. After the six standard positions measurement, the calibration factor ($X$) of the IMU sensor tool was:

$$X = \begin{pmatrix} 1.79783 & 0.31652 & 0.40881 \\ 0.17115 & 2.09477 & 0.13684 \\ -0.05037 & 0.50915 & 1.75151 \end{pmatrix}$$

and the bias or offset value of the IMU sensor tool was:

$$y = \begin{pmatrix} -0.2343 \\ -0.0593 \\ 0.1813 \end{pmatrix}$$

### 5.3 Filtering of Calibrating Acceleration Train Cabin Data

The calibration data of the acceleration train cabin data was filtered from noise using by Kalman Filter Method. The filtering process used MATLAB R2024b to help in the Standard Kalman filter calculation. The result of the calibration data of acceleration in the train cabin is shown in Figures 10 and 11.

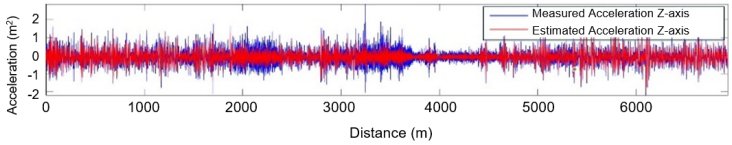


**Figure 10.** The filtered data of Z-axis acceleration data of the left railway track between Bandung to Rancaekek, Kilometer 161+000–KM 168+000

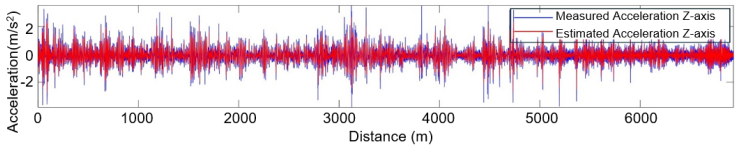


**Figure 11.** The filtered data of Z-axis acceleration data of the right railway track between Bandung to Rancaekek, Kilometer 161+000–Kilometer 168+000

### 5.4 Calculation of the Longitudinal Profile of the Railway Track Based on the Acceleration Data of the Train Cabin

Acceleration of train cabin data and longitudinal profile of railway track data must be synchronized because the sampling rate of data acquisition was different between the acceleration of train cabin data and the longitudinal profile of railway track data. Acceleration of train cabin data was recorded every 5 cm of railway track length, while the longitudinal profile of railway track data was recorded every 25 cm of railway track length.

The longitudinal profile of the railway track based on the acceleration data of the train cabin is shown in Figures 12 and 13.

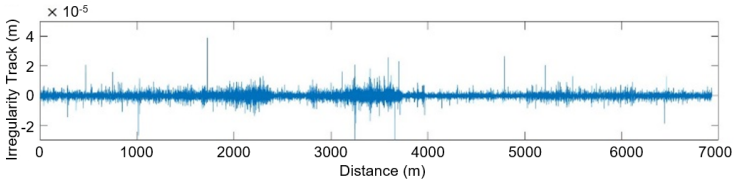


**Figure 12.** The longitudinal profile irregularity of the left-side railway track between Bandung to Rancaekek, Kilometer 161+000–Kilometer 168+000, based on the acceleration data of the train cabin

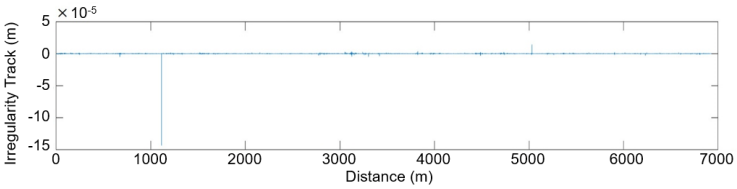


**Figure 13.** The longitudinal profile irregularity of the right-side railway track between Bandung to Rancaekek, Kilometer 161+000–Kilometer 168+000, based on the acceleration data of the train cabin

### 5.5 The Result of Normality Data Testing

If Z-axis accelerometer data in the train cabin were used to assess the longitudinal railway profile, it should be compared with the longitudinal profile railway data of the measuring geometry train. The sample rate of the IMU was set to 200 Hz, and the average speed of the train was 54 km/h or 15 m/s. Therefore, the corrected sampling

rate of the IMU was recorded every 7.5 cm. The vertical profile data of the TGMT data was recorded every 25 cm; therefore, the acceleration data from IMU and TGMT will align at 187.5 cm or every 1.875 m. The length of the track lane had been reviewed and was 7 km. Therefore, the total sample points that were possible to review were 3733 data. To synchronize IMU data and TGMT data, had used the formula "Vlookup(Lookup_value, Table_array, Col_index_num, Range_lookup)" in MS Excel.

The first stage of paired 2 dependent samples data testing was normally distributed data testing. If the paired 2 dependent sample data were normally distributed, use the Student T-test; however, if the paired 2 sample data were not normally distributed, use the Wilcoxon Signed Rank Test. The chart of normality data testing was done by Minitab Software Version 22 and was shown in Figures 14, 15, 16, and 17, and the summary of normality data testing was shown in Table 2.

**Table 2.** The summary of normality data testing

| Elevation Data | Mean | St. Dev. | P-Value |
|---|---|---|---|
| Longitudinal Profile Left Railway Track Based on Measurement | -0.00005754 | 0.003723 | <0.010 |
| Longitudinal Profile Left Railway Track Based on Acceleration Data Analysis | 1.28503E-08 | 0.00001327 | <0.010 |
| Longitudinal Profile Right Railway Track Based on Measurement | 0.00002227 | 0.003543 | <0.010 |
| Longitudinal Profile Right Railway Track Based on Acceleration Data Analysis | -5.74526E-09 | 0.0000017 | <0.010 |

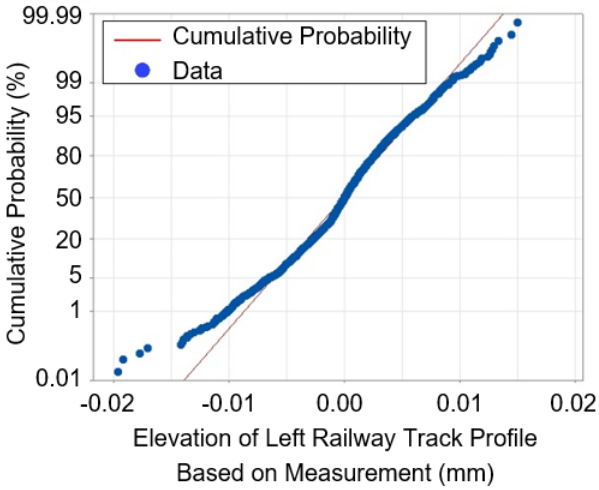


**Figure 14.** The result of normality data testing for the left rail of the longitudinal profile railway track data based on the TGMT

The longitudinal profile railway track data, based on the acceleration data of the train cabin, and the vertical profile railway track data based on the track geometry measuring trains, were not in normal distribution because the P-value was less than 0.05. Therefore, the statistical analysis used the Wilcoxon Signed Rank Test to compare the vertical profile of railway track data based on the acceleration data of the train cabin and the vertical profile of railway track data based on the TGMT.

### 5.6 The Wilcoxon Signed Rank Test's Null Hypothesis Testing Result

The study's goal was to investigate whether dynamic response in train cabins might be used to monitor the irregularity of longitudinal railway track. Therefore, the next analysis was a statistical comparison between the data from the longitudinal profile railway track data, which was based on the processing of the train cabin acceleration data, and the longitudinal profile railway track data, which was based on the TGMT.

The null hypothesis will be accepted if a P-value or asymptotic significance (2-tailed) value $> 0.05$ (5%). The Wilcoxon signed-rank test was done by Minitab Software Version 22, and the results were shown in Figures 18 and 19.

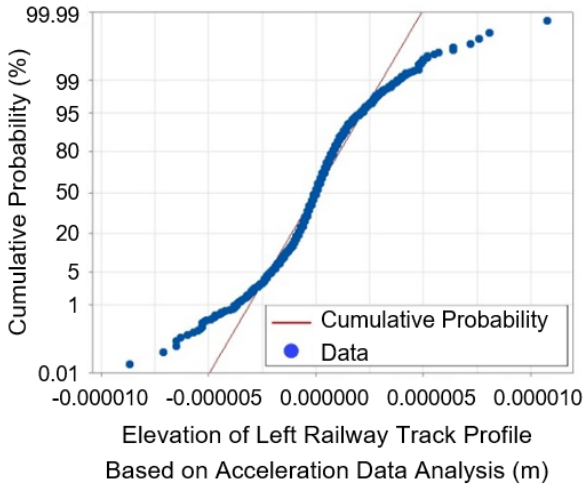


**Figure 15.** The result of normality data testing for the left rail of the longitudinal profile railway track data based on the acceleration data of the train cabin (IMU)

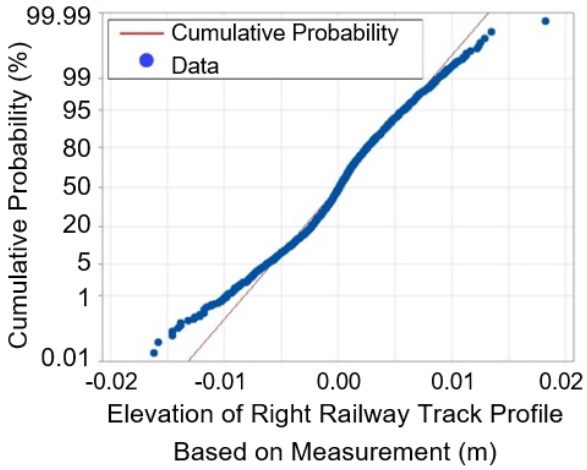


**Figure 16.** The result of normality data testing for the right rail of the longitudinal profile railway track data based on the TGMT

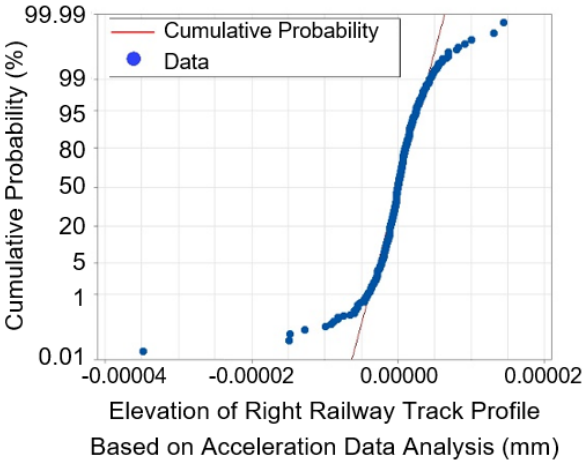


**Figure 17.** The result of normality data testing for the right rail of the longitudinal profile railway track data based on the acceleration data of the train cabin (IMU)

The result of the Wilcoxon Signed Ranks Test showed that the null hypothesis was accepted because the P-value

on the left rail was 0.725 and on the right rail was 0.073. All values of P-value were more than 0.05 (5%); the data of the longitudinal profile railway track, based on the processing of the train cabin acceleration data and based on the measurement of TGMT, were not different.

The longitudinal profile data were obtained from the measuring train in October 2022, and the accelerometer data from the IMU were obtained in January 2023. There was a 3-month difference between the TGMT data recording and the IMU acceleration data recording. Therefore, the P-value of the longitudinal profile of the right rail was 0.073, which approaches the threshold. This value, which is close to the minimum P-value, suggests that the irregularities of the railway were getting worse, or there were improvements to the longitudinal profile of the right rail.

**Test**

Null hypothesis $H_0$: $\eta = 0$
Alternative hypothesis $H_1$: $\eta \neq 0$

| Sample | N for Test | Wilcoxon Statistic | P-Value |
|---|---|---|---|
| Wilcoxon Test Left Rail | 3533 | 3142716.00 | 0.725 |

**Figure 18.** The result output of null hypothesis testing for the left rail of longitudinal profile railway track data, based on the acceleration data of the train cabin (IMU), and the longitudinal profile railway track data, based on TGMT by Minitab Software Version 22

**Test**

Null hypothesis $H_0$: $\eta = 0$
Alternative hypothesis $H_1$: $\eta \neq 0$

| Sample | N for Test | Wilcoxon Statistic | P-Value |
|---|---|---|---|
| Wilcoxon Test Right Rail | 3690 | 3521038.50 | 0.073 |

**Figure 19.** The result output of null hypothesis testing for the right rail of longitudinal profile railway track data, based on the acceleration data of the train cabin (IMU), and the longitudinal profile railway track data, based on TGMT by Minitab Software Version 22

The most common approach to analyzing effect size for a Wilcoxon signed-rank test was to calculate the rank biserial correlation coefficient ($r$), which can be obtained by dividing the Z-statistic by the square root of the sample size ($N$). In this research, the result of the rank biserial correlation coefficient calculation was 0.0000000281 for the left side of the longitudinal profile and 0.0000001437 for the right side of the longitudinal profile. The value of the rank biserial correlation coefficient was almost zero, which means the booth sizes of the longitudinal profile have given a very small effect on the Wilcoxon signed-rank test.

## 6 Conclusions

Currently, monitoring the geometric condition of railway tracks is still on the Track Geometric Measuring Train (TGMT). This research tries to develop a new method that is more efficient than usual, using dynamic response (acceleration) data within train cars. The sampling rate specification for the IMU sensor is to acquire data at a minimum of 25 cm at a train speed of 100 km/h. It is recommended to use an IMU sensor with a sampling rate of 200 Hz, while also considering the analysis of noise measurement.

The result of the analysis is no difference between the vertical profile railway data based on the acceleration data of the train cabin and the vertical profile railway data based on the measuring geometry train, because the result of the Wilcoxon Signed Ranks Test showed the null hypothesis accepted. After all, the P-value on the left rail is 0.725, and on the right rail is 0.073, which is greater than 0.05 (5%). Since there is no difference between the railway profile based on the TGMT and the longitudinal profile of railway data based on the acceleration data of the train

cabin, the dynamic response in the train cabin could be able monitor the longitudinal profile of railways. The results of this research apply to trains using the same type of train bogie that was used to collect acceleration data. The type of train bogie was Bogie NT-11 (K-5).

The next study can be proposed, which involves monitoring the longitudinal profile of the railway track with a longer track segment or the lateral profile of the railway track by using dynamic response data in the train cabin, or proposing a mathematical model of the relationship between the dynamic response in the train cabin and the quality of the railway track. Further research should also consider that the time interval between TGMT measurements and IMU measurements should not be too long.

## Author Contributions

Conceptualization, I. and H.W.; methodology, I. and H.W.; software, I.; validation, I. and H.W.; formal analysis, I. and H.W.; investigation, I. and H.W.; resources, I. and H.W.; data curation, I. and H.W.; writing—original draft preparation, I.; writing—review and editing, I. and H.W.; visualization, I.; supervision, H.W.; project administration, I. All authors have read and agreed to the published version of the manuscript.

## Data Availability

The data used to support the findings of this study are available from the corresponding author upon request.


## Acknowledgements

We would like to thank the Education Fund Management Institute (LPDP), the Finance Ministry of the Republic of Indonesia for providing research funding for the 2017 Indonesian Lecturer Scholarship (BUDI) doctoral program.


## Conflicts of Interest

The authors declare that they have no conflicts of interest.

## References


[1] D. Ristić-Durrant, M. Franke, and K. Michels, "A review of vision-based on-board obstacle detection and distance estimation in railways," *Sensors*, vol. 21, no. 10, p. 3452, 2021. https://doi.org/10.3390/s21103452

[2] D. Šemrov, A. Pavšek, and F. Zemljič, "Railway as the solution for road congestion," in *2nd International Conference on Road and Rail Infrastructure, Dubrovnik, Croatia*, 2012, pp. 601–605.

[3] A. Utami and H. Widyastuti, "Study of society behaviour to early warning in the railway level crossing without barrier in Gayungsari, Surabaya," *J. Ind. Res. Innov.*, vol. 14, no. 1, pp. 39–46, 2020. https://doi.org/10.29122/mipi.v14i1.4040

[4] S. N. Lingamanaik, C. Thompson, N. Nadarajah, R. Ravitharan, H. Widyastuti, and W. K. Chiu, "Using instrumented revenue vehicles to inspect track integrity and rolling stock performance in a passenger network during peak times," *Procedia Eng.*, vol. 188, pp. 424–431, 2017. https://doi.org/10.1016/j.proeng.2017.04.504

[5] A. Y. Nurhidayat, H. Widyastuti, Sutikno, and D. P. Upahita, "Research on passengers preferences and impact of high-speed rail on air transport demand," *Sustainability*, vol. 15, no. 4, p. 3060, 2023. https://doi.org/10.3390/su15043060

[6] B. Rahardjo, I. B. Mochtar, and H. Widyastuti, "The effect of level crossing on the railroad line capacity," *Civ. Eng. Archit.*, vol. 10, no. 6, pp. 2491–2499, 2022. https://doi.org/10.13189/cea.2022.100620

[7] H. Widyastuti and A. F. Sedayu, "Comparison analysis of indonesian railway track quality index calculation results with European Standards (EN) using multibody dynamic system simulation results (case study: DAOP VIII Lawang-Malang)," in *30th International Conference on Noise and Vibration Engineering, ISMA 2022 and 9th International Conference on Uncertainty in Structural Dynamics, USD 2022, Leuven, Belgium*, 2022, pp. 3341–3354.

[8] D. M. Setiawan and S. A. P. Rosyidi, "Track quality index as track quality assessment indicator," in *Simposium XIX FSTPT*, 2016, pp. 11–13.

[9] E. J. Obrien, C. Bowe, and P. Quirke, "Determination of longitudinal profile of railway track using vehicle-based inertial readings," *Proc. Inst. Mech. Eng. Part F J. Rail Rapid Transit*, vol. 231, no. 5, pp. 518–534, 2016. https://doi.org/10.1177/0954409716664936

[10] A. Malekjafarian, C. A. Sarrabezolles, and M. A. A. Khan, "Machine-learning-based approach for railway track monitoring using acceleration measured on an in-service train," *Sensors*, vol. 23, no. 17, p. 7568, 2023. https://doi.org/10.3390/s23177568

[11] P. F. Weston, C. S. Ling, C. Roberts, C. J. Goodman, P. Li, and R. M. Goodall, "Monitoring vertical track irregularity from in-service railway vehicles," *Proc. Inst. Mech. Eng. Part F J. Rail Rapid Transit*, vol. 221, no. 1, pp. 75–88, 2006. https://doi.org/10.1243/0954409JRRT65

[12] Ministry of Transportation of the Republic of Indonesia, "Transportation Statistic Operational Data 2022," 2022. https://www.dephub.go.id/post/read/buku-statistik-data-operasional-tahun-2022

[13] X. Liu, M. R. Saat, and C. P. L. Barkan, "Analysis of causes of major train derailment and their effect on accident rates," *Transp. Res. Rec. J. Transp. Res. Board*, vol. 2289, no. 1, pp. 154–163, 2012. https://doi.org/10.3141/2289-20

[14] A. Jamshidi, S. F. Roohi, A. Núñez, R. Babuska, B. De Schutter, R. Dollevoet, and Z. Li, "Probabilistic defect-based risk assessment approach for rail failures in railway infrastructure," *IFAC-PapersOnLine*, vol. 49, no. 3, pp. 73–77, 2016. https://doi.org/10.1016/j.ifacol.2016.07.013

[15] I. A. Faisal, T. W. Purboyo, and A. S. R. Ansori, "A review of accelerometer sensor and gyroscope sensor in IMU sensors on motion capture," *J. Eng. Appl. Sci.*, vol. 15, no. 3, pp. 826–829, 2020. https://doi.org/10.36478/jeasci.2020.826.829

[16] B. Fang, F. Sun, H. Liu, and C. Liu, "3D human gesture capturing and recognition by the IMMU-based data glove," *Neurocomputing*, vol. 277, pp. 198–207, 2018. https://doi.org/10.1016/j.neucom.2017.02.101

[17] A. Chudzikiewicz, R. Bogacz, M. Kostrzewski, and R. Konowrocki, "Condition monitoring of railway track systems by using acceleration signals on wheelset axle-boxes," *J. Transport*, vol. 33, no. 2, pp. 555–566, 2018. https://doi.org/10.3846/16484142.2017.1342101

[18] J. I. Real, L. Montalbán-Dominggo, T. Real, and V. Puig, "Development of a system to obtain vertical track geometry measuring axle-box accelerations from in-service trains," *J. Vibroeng.*, vol. 14, no. 2, pp. 813–826, 2012.

[19] P. Quirke, E. OBrien, C. Bowe, A. Malekjafarian, and D. Cantero, "Estimation of railway track longitudinal profile using vehicle-based inertial measurements," in *Sustainable Solutions for Railways and Transportation Engineering. GeoMEast 2018. Sustainable Civil Infrastructures*. Cham: Springer, 2018, pp. 145–148. https://doi.org/10.1007/978-3-030-01911-2_1

[20] J. C. Groos, P. Havrila, and L. A. Schubert, "In-service railway track condition monitoring by analysis of axle box accelerations for small to mid-size infrastructure operators," *Cond. Monit.*, vol. 376, pp. 5–9, 2018.

[21] Z. Xing, Y. Chen, and Y. Qing, "On-line monitoring of vertical long wavelength track irregularities using bogie pitch rate," *J. Vibroeng.*, vol. 17, no. 1, pp. 216–228, 2015.

[22] E. J. OBrien, P. Quirke, C. Bowe, and D. Cantero, "Determination of railway track longitudinal profile using measured inertial response of an in-service railway vehicle," *Struct. Health Monit.*, vol. 17, no. 6, pp. 1425–1440, 2017. https://doi.org/10.1177/1475921717744479

[23] C. Chellaswamy, S. Duraichamy, P. Glaretsubin, and A. Vanathi, "Optimized vehicle acceleration measurement for rail track condition monitoring," in *2nd International Conference on Computing and Communications Technologies (ICCCT), Chennai, India*, 2017, pp. 155–160. https://doi.org/10.1109/ICCCT2.2017.7972265

[24] N. Nadarajah, A. Shamdani, G. Hardie, W. K. Chiu, and H. Widyastuti, "Prediction of railway vehicles' dynamic behavior with machine learning algorithms," *Electron. J. Struct. Eng.*, vol. 18, no. 1, pp. 38–46, 2018. https://doi.org/10.56748/ejse.182271

[25] J. Sadeghi, H. Heydari, and E. A. Doloei, "Improvement of railway maintenance approach by developing a new railway condition index," *J. Transp. Eng. Part A Syst.*, vol. 143, no. 8, pp. 04 017 037–1–04 017 037–10, 2017. https://doi.org/10.1061/JTEPBS.0000063

[26] R. Wawryszczuk, E. Kardas-Cinal, J. Lejk, and M. Sokolowski, "Methods of passenger ride comfort evaluation—Tests for metro cars," *Sensors*, vol. 23, no. 12, p. 5741, 2023. https://doi.org/10.3390/s23125741

[27] O. Woodman, "An introduction to inertial navigation," 2007, University of Cambridge, UCAM-CL-TR-696. https://doi.org/10.48456/tr-696

[28] I. Georgieva, C. Hofreither, T. Ilieva, and S. Nakov, "Laboratory calibration of a MEMS accelerometer sensor," 2013, European Study Group with Industry, 633.

[29] A. Ma'arif, A. Iswanto, A. Nuryono, and R. I. Alfiand, "Kalman filter for noise reducer on sensor readings," *Signal Image Process. Lett.*, vol. 1, no. 2, pp. 50–61, 2019. https://doi.org/10.31763/simple.v1i2.2

[30] R. E. Kalman, "A new approach to linear filtering and prediction problems," *J. Fluids Eng. Trans. ASME*, vol. 82, no. 1, pp. 35–45, 1960. https://doi.org/10.1115/1.3662552

[31] Y. Wu, Y. Sui, and G. Wang, "Vision-based real-time aerial object localization and tracking for UAV sensing system," *IEEE Access*, vol. 5, pp. 23 969–23 978, 2017. https://doi.org/10.1109/ACCESS.2017.2764419

[32] Lasmadi, A. Cahyadi, S. Herdjunanto, and R. Hidayat, "Inertial navigation for quadrotor using Kalman filter with drift compensation," *Int. J. Electron. Comput. Eng.*, vol. 7, no. 5, pp. 2596–2604, 2017. https://doi.org/10.11591/ijece.v7i5.pp2596-2604

[33] N. G. M. Thao, D. H. Nghia, and N. H. Phuc, "A PID backstepping controller for two-wheeled self-balancing robot," in *International Forum on Strategic Technology (IFOST), Ulsan, South Korea*, 2010, pp. 76–81.

https://doi.org/10.1109/IFOST.2010.5668001

[34] S. Nurmaini and S. Pangidoan, "Localization of leader-follower robot using extended Kalman filter," *Comput. Eng. Appl. J.*, vol. 7, no. 2, pp. 95–108, 2018. https://doi.org/10.18495/comengapp.v7i2.253

[35] H. Khazraj, F. F. Da Silva, and C. L. Bak, "A performance comparison between extended Kalman filter and unscented Kalman filter in power system dynamic state estimation," in *51st International Universities Power Engineering Conference (UPEC), Coimbra, Portugal*, 2016, pp. 1–6. https://doi.org/10.1109/UPEC.2016.8114125

[36] S. Afrasiabi, M. Afrasiabi, M. Rastegar, M. Mohammadi, B. Parang, and F. Ferdowsi, "Ensemble Kalman filter based dynamic state estimation of PMSG-based wind turbine," in *IEEE Texas Power and Energy Conference (TPEC), College Station, TX, USA*, 2019, pp. 1–4. https://doi.org/10.1109/TPEC.2019.8662174

[37] D. W. Kim and C. S. Park, "Application of Kalman filter for estimating a process disturbance in a building space," *Sustainability*, vol. 9, no. 10, p. 1868, 2017. https://doi.org/10.3390/su9101868

[38] B. B. Guo and Y. Yuan, "A comparative review of methods for comparing means using partially paired data," *Stat. Methods Med. Res.*, vol. 26, no. 3, pp. 1323–1340, 2015. https://doi.org/10.1177/0962280215577111

[39] M. Prabhaker, U. Singh, C. M. Pandey, P. Mishra, and G. Pandey, "Application of student's t-test, analysis of variance, and covariance," *Ann. Card. Anesth.*, vol. 22, no. 4, pp. 407–411, 2019. https://doi.org/10.4103/aca.ACA_94_19

[40] S. M. Taheri and H. Gholamreza, "A generalization of the Wilcoxon signed-rank test and its applications," *Stat. Pap.*, vol. 54, pp. 457–470, 2013. https://doi.org/10.1007/s00362-012-0443-4